Topological Electromagnetic Effects and Higher Second Chern Numbers in Four-Dimensional Gapped Phases

Yan-Qing Zhu,[1,*] Zhen Zheng,[2,3] Giandomenico Palumbo,[4,†] and Z. D. Wang[1,‡]

[1]*Guangdong-Hong Kong Joint Laboratory of Quantum Matter, Department of Physics, and HKU-UCAS Joint Institute for Theoretical and Computational Physics at Hong Kong, The University of Hong Kong, Pokfulam Road, Hong Kong, China*

[2]*Guangdong-Hong Kong Joint Laboratory of Quantum Matter, Frontier Research Institute for Physics, South China Normal University, Guangzhou 510006, China*

[3]*Guangdong Provincial Key Laboratory of Quantum Engineering and Quantum Materials, School of Physics and Telecommunication Engineering, South China Normal University, Guangzhou 510006, China*

[4]*School of Theoretical Physics, Dublin Institute for Advanced Studies, 10 Burlington Road, Dublin 4, Ireland*

(Received 7 April 2022; revised 29 September 2022; accepted 19 October 2022; published 4 November 2022)

Higher-dimensional topological phases play a key role in understanding the lower-dimensional topological phases and the related topological responses through a dimensional reduction procedure. In this work, we present a Dirac-type model of four-dimensional $\mathbb{Z}_2$ topological insulator (TI) protected by $\mathcal{CP}$ symmetry, whose 3D boundary supports an odd number of Dirac cones. A specific perturbation splits each bulk massive Dirac cone into two valleys separated in energy-momentum space with opposite second Chern numbers, in which the 3D boundary modes become a nodal sphere or a Weyl semimetallic phase. By introducing the electromagnetic (EM) and pseudo-EM fields, exotic topological responses of our 4D system are revealed, which are found to be described by the $(4+1)$D mixed Chern-Simons theories in the low-energy regime. Notably, several topological phase transitions occur from a $\mathcal{CP}$-broken $\mathbb{Z}_2$ TI to a $\mathbb{Z}$ TI when the bulk gap closes by giving rise to exotic double-nodal-line or nodal-hyper-torus gapless phases. Finally, we propose to probe experimentally these topological effects in cold atoms.

DOI: 10.1103/PhysRevLett.129.196602

Introduction.—The prediction and discovery of topological insulators (TIs) and topological semimetals (TSMs) has led to an explosion of activity in studying topological aspects of band structures in the past decade. Nowadays, topological phases of matter have been at the forefront of the condensed matter and artificial systems [1–8]. One reason for the excitement is that these topological phases beyond Landau's spontaneous symmetry breaking theory are protected by certain symmetries which support nontrivial boundary states associated with a topological invariant in the bulk. Another significant feature relies on their corresponding topological electromagnetic (EM) responses which are described by topological field theories. For instance, the $(2+1)$-D Chern-Simons theory describes the quantum anomalous Hall effect in 2D Chern insulators [9], the $(3+1)$D axion field theory describes the magnetoelectric effect in 3D $\mathbb{Z}_2$ TIs [10], and the $(3+1)$D mixed axion theory [11] describes the EM response in certain 3D topological crystalline insulators [12]. Similarly, TSMs also exhibit topological transport phenomena described by the mixed Chern-Simons or axion theory [13–17] and can be understood via quantum anomalies [18], such as parity anomaly in 2D and 4D TSMs [19,20], chiral anomaly in 3D Weyl semimetals [21,22], and $\mathbb{Z}_2$ and chiral anomalies in 3D Dirac semimetals [23].

On the other hand, higher-dimensional topological phases (HDTPs) are much less explored due to their impossible realization in solid-state materials. However, 4D topological phases can be implemented in synthetic matter as recently shown in Refs. [24–30]. Moreover, HDTPs play an important theoretical role in lower-dimensional topological phases. For instance, the well-known 2D and 3D TIs can be obtained from a 4D time-reversal-invariant (TRI) insulator through dimensional reduction as well as their effective field-theoretical descriptions [10]. The 3D boundaries of such a $\mathbb{Z}$-class 4D TI supports an odd number of Weyl points with the same chirality which cannot be realized in any 3D systems due to the Nielsen-Ninomiya no-go theorem. Inspired by this idea, one may wonder: *Does there exist a 4D TI phase that supports an odd number of different types of nodal structures on its 3D boundaries? Are there novel topological responses if this system does exist?*

In this Letter, we answer positively to both questions. We first present a $\mathbb{Z}_2$ 4D TI model that supports an odd number of real Dirac points on its 3D boundary normal to the fourth dimensions, which are protected by $\mathcal{CP}$ symmetry beyond the tenfold way classification [31]($\mathcal{C}$ and $\mathcal{P}$ denote particle-hole and inversion symmetries, respectively). The bulk $\mathbb{Z}_2$ invariant ν_2 can be defined by the second spin Chern number (CN), i.e., the higher-dimensional generalization of

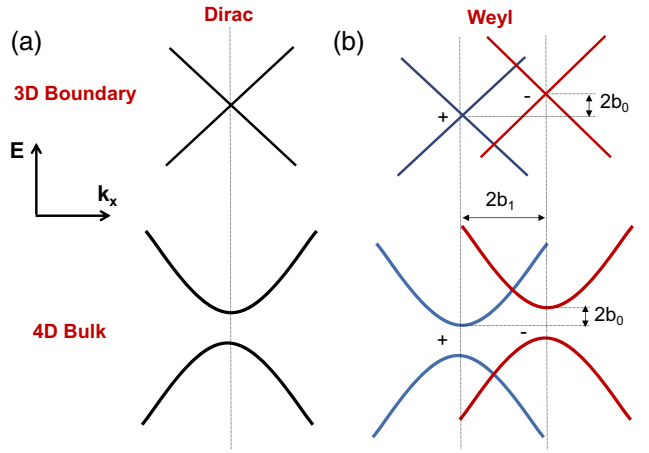

FIG. 1. Schematic of low-energy spectra for $2 < m < 4$ near $k = 0$. (a) (upper panel) A real Dirac cone as a boundary state on the 3D boundary when considering open boundary condition along the w direction, while a double massive Dirac cone as the bulk spectrum is presented in the bottom panel. (b) Upper (bottom) panel shows that vector field b_μ lifts the degeneracy of the 3D boundary massless (4D bulk massive) Dirac cone which induces two Weyl points (valleys) with opposite chirality (second CN) separated in energy and in momentum with difference $2b_0$ and $2b_1$, respectively.

the spin CN in 2D TRI insulators without spin-orbit-coupling (SOC). Subsequently, we will introduce a perturbation which will break the degeneracy of the bulk spectrum forming two valleys with opposite second CNs. In this case ν_2 remains unchanged and is associated with the second valley CN which is defined as the half difference of the second CNs for two valley indices instead of "spin." On the 3D boundary, each real Dirac point will split into two Weyl points with opposite chirality in the separation of energy forming a Weyl nodal sphere or of momentum forming a Weyl semimetallic phase, see Fig. 1. Moreover, we will show that such a $\mathbb{Z}_2$ phase has some novel electromagnetic responses upon applying the EM and pseudo-EM fields [22,32–34]. The field theoretical-description of "*4D quantum spin Hall effect*" in our model is also developed. We identify two novel quantum effects, coined, "*valley-induced electromagnetic effect*," and "*4D quantum valley Hall effect*." These bulk responses are consistent with the anomaly equations of the 3D boundary Dirac or Weyl modes arising from the $\mathbb{Z}_2$ or chiral anomaly. Furthermore, we explore several types of topological phase transitions from a $\mathbb{Z}_2$ TI to a $\mathbb{Z}$ TI where the phase transition occurs only when a bulk gap closes. We will show that there are many exotic topological phases that appear during the transition processes including the double-nodal-line (DNL) and nodal-hyper-torus (NHT) semimetallic phases and the 4D quantum Hall insulator (QHI) phases with higher second CNs. Finally, we will propose to realize such a 4D model and to detect the predicted responses in a 3D optical lattice with an extra periodic parameter using ultracold atoms.

Model and bulk topology.—Let us start with the minimal model of a 4D $\mathbb{Z}_2$ TI which takes the form,

$$\mathcal{H}_0(k) = d_x\Gamma_1 + d_y\Gamma_2 + d_z\Gamma_3 + d_w\Gamma_4 + d_m\Gamma_0, \quad (1)$$

with the Bloch vector being $d_i = \sin k_i$ and $d_m = m - \sum_i \cos k_i$ with $i = x,\ y,\ z,\ w$. The 8×8 matrices Γ_i satisfying a Clifford algebra are presented in Ref. [35]. This system hosts two fourfold degenerate bands with the spectrum, $E_\pm = \pm\sqrt{d_x^2 + d_y^2 + d_z^2 + d_w^2 + d_m^2}$.

This model preserves the $\mathcal{CP}$ symmetry, i.e., $\{\mathcal{CP}, \mathcal{H}_0\} = 0$, with $\mathcal{CP} = iG_{112}\mathcal{K}$ satisfying $(\mathcal{CP})^2 = -1$. We label $G_{ijk} = \sigma_i \otimes \sigma_j \otimes \sigma_k$ hereafter and $\mathcal{K}$ as the complex conjugate operator. Thus this system is characterized by a $\mathbb{Z}_2$ invariant [36]. We next move to discuss the bulk topology of this system. The Hamiltonian commutes with a matrix $\Gamma_5 = G_{332}$, i.e., $[\Gamma_5, \mathcal{H}_0] = 0$. It implies that this model can be block diagonalized after rotating Γ_5 into G_{300} through a unitary matrix $U = \exp[-(i\pi/4)G_{100}]\exp[(i\pi/4)G_{132}]$, and is written in the form of $\mathcal{H}_{BD} = U\mathcal{H}_0U^{-1} = \mathcal{H}_+ \oplus \mathcal{H}_-$, where each block Hamiltonian is given by

$$\mathcal{H}_\pm(k) = -d_xG_{33} + d_yG_{10} - d_zG_{31} - d_wG_{20} \pm d_mG_{32}, \quad (2)$$

with $G_{ij} = \sigma_i \otimes \sigma_j$.

$\mathcal{H}_{BD}$ preserves $\mathcal{CP}$ symmetry with $\mathcal{CP} = iG_{120}\mathcal{K}$. Although $\mathcal{H}_\pm$ breaks $\mathcal{CP}$ symmetry, each block Hamiltonian preserves the time-reversal-symmetry (TRS) and thus falls into class AII with $\mathcal{T} = iG_{20}\mathcal{K}$ satisfying $\mathcal{T}^2 = -1$. Therefore, each block model is a 4D QHI characterized by the second CN [10],

$$C_2^\pm = \frac{1}{32\pi^2}\int_{\mathbb{T}^4} d^4k\, \epsilon^{\mu\nu\rho\sigma}\mathrm{tr}(\mathcal{F}^\pm_{\mu\nu}\mathcal{F}^\pm_{\rho\sigma}), \quad (3)$$

with the values $C_2^\pm = \pm 3\mathrm{sgn}(m)$ for $0 < |m| < 2$, $C_2^\pm = \mp\,\mathrm{sgn}(m)$ for $2 < |m| < 4$, and $C_2^\pm = 0$ elsewhere. Here the non-Abelian Berry curvature $\mathcal{F}^\pm_{\mu\nu} = \partial_\mu\mathcal{A}^\pm_\nu - \partial_\nu\mathcal{A}^\pm_\mu - i[\mathcal{A}^\pm_\mu, \mathcal{A}^\pm_\nu]$, where $(\mathcal{A}^\pm_\mu)^{\alpha\beta} = i\langle u^\pm_\alpha|\partial_\mu|u^\pm_\beta\rangle$ denotes the non-Abelian Berry connection defined by the occupied eigenstates $|u^\pm_\alpha\rangle$ of each block (we set the Fermi energy at $\epsilon_F = 0$). Therefore, although the total second CN is zero, namely, $C_2 = C_2^+ + C_2^- = 0$, we can define a $\mathbb{Z}_2$ number given by

$$\nu_2 = C_{2s} \bmod 2, \quad (4)$$

with the second spin CN [37] being $C_{2s} = (C_2^+ - C_2^-)/2$ which can be regarded as a generalization of the first spin CN in a 2D TRI system without SOC. Note that one can also define the $\mathbb{Z}_2$ number ν_2 in terms of the Green's function for the original model $\mathcal{H}_0$ [38].

This system enjoys more extra symmetries [39], e.g., $\mathcal{RT}$, mirror, time-reversal, particle-hole, and chiral symmetries; see Supplemental Material [39] for details. Thus it implies that this model will host a very rich phase diagram when we introduce some extra symmetry-protected or broken perturbations. In the following part, we mainly focus on the $\mathbb{Z}_2$ topological phases and discuss the perturbations that commuting with Γ_5 which means these terms can be block diagonalized, i.e., ν_2 is still well defined and unchanged unless there is a gap closing phase transition in the bulk. For concreteness, we introduce the $\mathcal{CP}$-broken but Γ_5-protected perturbation,

$$\Delta = \Gamma_5\left(b_0 + \sum_{i=1}^{3} b_i\Gamma_i\right). \tag{5}$$

Boundary physics.—Without loss of generality, we mainly address the 3D boundary physics by considering a boundary perpendicular to the w direction with a lattice length L_w. The cases for open boundary conditions along the other directions are presented in the Supplemental Material [39]. Now let us first focus on the case of $\mathcal{H}_0$ where $2 < m < 4$ and thus $C_2^{\pm} = \mp 1$. The effective boundary Hamiltonian at $L = 0$ is given by $\mathcal{H}_{\text{eff}} = -\sin k_x G_{13} + \sin k_y G_{30} - \sin k_z G_{11}$. It supports a real Dirac point at the origin with the expanded Hamiltonian,

$$\mathcal{H}_{RD}(\mathbf{k}) = -k_x G_{13} + k_y G_{30} - k_z G_{11}. \tag{6}$$

Note that this model preserves $\mathcal{PT}$ symmetry, i.e., $[\mathcal{PT}, \mathcal{H}_{RD}] = 0$, with $\mathcal{PT} = \mathcal{K}$ satisfying $(\mathcal{PT})^2 = +1$. Thus this model presents a real Dirac monopole with a $\mathbb{Z}_2$ classification and carries a monopole charge $\nu_R = 1$ defined in terms of the real CN [53] or the first Euler number [54–56]. Moreover, one can see that a real Dirac point consists of two Weyl points with opposite chirality under the rotation representation [57].

Next we add the above-mentioned term Δ to $\mathcal{H}_0$, i.e., $\mathcal{H}_1 = \mathcal{H}_0 + \Delta$. The system now hosts two Dirac valleys with energy and momentum differences $\delta E = 2b_0$ and $\delta k = 2\mathbf{b}$ in the bulk, respectively, see Fig. 1. In the block diagonal representation, each block Hamiltonian still hosts the unchanged second CN $C_2^{\pm}$ and thus we have $\nu_2 = C_{2v} \bmod 2$ with $C_{2v} = C_{2s}$ which is nothing but the second valley CN. To be more clear, we first discuss the case when only b_0 is nonzero. Now the total low-energy 3D boundary Hamiltonian becomes

$$\mathcal{H}_{NS}(\mathbf{k}) = \mathcal{H}_{RD}(\mathbf{k}) + b_0\gamma_5, \tag{7}$$

with $\gamma_5 = G_{32}$. Note that γ_5 commutes with $\mathcal{H}_{RD}$, i.e., $[\gamma_5, \mathcal{H}_{RD}] = 0$. This model represents a 3D Weyl nodal sphere with spectrum $E_{\pm} = \pm|\mathbf{k}| \pm |b_0|$, exhibiting a band degeneracy at the Fermi level $E = 0$ on a sphere defined by $|\mathbf{k}| = |b_0|$ with $|\mathbf{k}| = \sqrt{k_x^2 + k_y^2 + k_z^2}$. This model breaks $\mathcal{PT}$ but keeps the γ_5 symmetry, and thus the nodal sphere carries a $\mathbb{Z}$ monopole charge [58,59].

In the case when only $\mathbf{b} = (b_1, b_2, b_3)$ is nonzero, we obtain a Weyl semimetallic phase on its 3D boundary with the low-energy effective Hamiltonian given by

$$\mathcal{H}_{WS} = \mathcal{H}_{RD}(\mathbf{k}) + b_1 G_{21} + b_2 G_{02} + b_3 G_{23}. \tag{8}$$

Its spectrum reads $E_{\pm} = \pm\sqrt{(k_x \pm b_1)^2 + (k_y \pm b_2)^2 + (k_z \pm b_3)^2}$, which represents a pair of Weyl points with opposite charge or chirality at $\mathbf{k}_W^{\pm} = \pm(b_1, b_2, b_3)$.

In other words, the 3D boundary physics of $\mathcal{H}_1$ describes a pair of Weyl points with opposite chirality separated in energy-momentum space with $\delta E = 2b_0$ and $\delta\mathbf{k} = 2\mathbf{b}$, as shown in Fig. 1. Generally, there are $|C_{2v}|$ gapless boundary modes on its 3D boundary when m varies in different regions [60]. Notice that the 2D (0D) topological charge implies that the boundary band structure with an odd number of real Dirac points (nodal spheres) cannot be realized by any 3D systems, and it can only exist at the boundary of a 4D gapped system.

Topological responses.—For later convenience, we here consider the simplest case in the block diagonal representation, i.e., $\mathcal{H}_{BD}$. To calculate the continuum response we couple each continuum Hamiltonian with its own gauge field $A_\mu^{(a)}$ via $k_\mu \to k_\mu + A_\mu^{(a)}$. The topological action of the 4D QHI in each block is described by the $(4+1)$D Chern-Simons theory [10], i.e.,

$$S_{\text{eff}}^{(a)} = \frac{C_2^{(a)}}{24\pi^2}\int d^5k\, \epsilon^{\mu\nu\lambda\rho\sigma} A_\mu^{(a)} \partial_\nu A_\lambda^{(a)} \partial_\rho A_\sigma^{(a)}, \tag{9}$$

where $a = \pm$ for each block, and $A_\mu = \frac{1}{2}[A_\mu^{(+)} + A_\mu^{(-)}]$, $\tilde{A}_\mu = \frac{1}{2}[A_\mu^{(+)} - A_\mu^{(-)}]$. The symmetric combination of the gauge fields $A_\mu^{(+)}$ and $A_\mu^{(-)}$ represents the usual EM field A_μ; while the antisymmetric combination is a spin gauge field $\tilde{A}_\mu$, such that we obtain a new kind of mixed Chern-Simons action,

$$\begin{aligned} S_{\text{eff}} = {} & \frac{C_{2s}}{4\pi^2}\int d^5x\, \epsilon^{\mu\nu\lambda\rho\sigma} \tilde{A}_\mu \partial_\nu A_\lambda \partial_\rho A_\sigma \\ & + \frac{C_{2s}}{12\pi^2}\int d^5x\, \epsilon^{\mu\nu\lambda\rho\sigma} \tilde{A}_\mu \partial_\nu \tilde{A}_\lambda \partial_\rho \tilde{A}_\sigma. \end{aligned} \tag{10}$$

This action can also be derived in a direct diagrammatic calculation by evaluating the diagram [20,61]. Varying it with respect to A_μ and $\tilde{A}_\mu$, respectively, we obtain the corresponding charge and spin currents, i.e., $J^\mu = \delta S_{\text{eff}}/\delta A_\mu$, and $\tilde{J}^\mu = \delta S_{\text{eff}}/\delta \tilde{A}_\mu$. For instance, considering a simple field configuration,

$$\tilde{A}_\mu = 0, \qquad A_\mu = (-zE_z, -yB_z, 0, 0, 0), \tag{11}$$

we obtain

$$J^w = 0, \qquad \tilde{J}^w = \frac{C_{2s}}{4\pi^2} E_z B_z. \tag{12}$$

Here $\mathbf{E}$ and $\mathbf{B}$ denote the components of the usual EM field defined later. $\tilde{J}^w$ denotes the spin current upon applying an EM field which can be regarded as the *4D quantum spin Hall effect*. Note that the index spin above may also include but is not limited to the following internal degree of freedom of different physical objects, e.g., hyperstates and orbits of atoms, etc.

The above results can actually be understood by connecting to the 2D cases [39]. Integrating over x, y dimensions with periodic boundary conditions and assuming E_z does not depend on (x, y), we have

$$\int dxdy\, \tilde{J}^w = \frac{C_{2s}}{2\pi} N_{xy} E_z, \tag{13}$$

where $N_{xy} = \int dxdy\, B_z/2\pi$ denotes the number of flux quanta through the xy plane, which is always quantized to be an integer. Thus, we can understand this result in a $\mathbb{Z}_2$ $(4+1)$D insulator with the second spin CN C_{2s}. This formula denotes the quantum spin Hall effect with a spin Hall conductance $C_{2s}N_{xy}/2\pi$ in the zw plane induced by a magnetic field with flux $2\pi N_{xy}$ in the normal xy plane.

On the other hand, since this model supports $|C_{2s}|$ Dirac cones on its 3D boundary, we can explore the 3D boundary response properties from the bulk. Integrating out with respect to w [picking the gauge as Eq. (11)] in S_{eff}, we obtain the boundary term

$$S_{BD} = \frac{C_{2s}}{12\pi^2} \int d^4x\, \epsilon^{\mu\nu\rho\sigma} (3\tilde{A}_\mu A_\nu \partial_\rho A_\sigma + \tilde{A}_\mu \tilde{A}_\nu \partial_\rho \tilde{A}_\sigma), \tag{14}$$

where $\mu = t, x, y, z$. The corresponding currents are given by

$$j^z = 0, \qquad \tilde{j}^z = \frac{C_{2s}}{4\pi^2} z E_z B_z. \tag{15}$$

After varying above currents with respect to z, we obtain $\partial_z j^z = J^w$ and $\partial_z \tilde{j}^z = \tilde{J}^w$ are the same as those presented in Eq. (12). This result can be also directly derived from the boundary Dirac Hamiltonian [39]. We emphasize that such a nonzero spin current $\tilde{j}^z$ only appears on the boundary of 4D $\mathbb{Z}_2$ TIs which stems from the odd number of (real) Dirac cone structure that cannot be realized by any 3D systems [53].

In what follows we consider the case of $\mathcal{H}_1$. By coupling each block Hamiltonian with $A_\mu^{(\pm)}$ via $k_\mu \to k_\mu + A_\mu^{(\pm)}$ and treating b_μ as an axial gauge field with $A_\mu^{(\pm)} = A_\mu \pm b_\mu$, where $b_\mu = (b_0, \mathbf{b}, 0)$, we have $b_\mu \equiv A_\mu^5 = \frac{1}{2}[A_\mu^{(+)} - A_\mu^{(-)}]$. Consequently, we obtain the effective action just by replacing $\tilde{A}_\mu$ with b_μ, i.e.,

$$S_{v,\text{eff}} = \frac{C_{2v}\epsilon^{\mu\nu\lambda\rho\sigma}}{12\pi^2} \int d^5x (3b_\mu \partial_\nu A_\lambda \partial_\rho A_\sigma + b_\mu \partial_\nu b_\lambda \partial_\rho b_\sigma). \tag{16}$$

Note that this bulk response matches with the EM response of a 4D topological semimetal that hosts two 4D monopoles separated in energy-momentum space where we find precisely half of coefficient occurs [20,61]. The corresponding charge and valley currents are derived from $J^\mu = \delta S_{v,\text{eff}}/\delta A_\mu$ and $J_5^\mu = \delta S_{v,\text{eff}}/\delta b_\mu$, respectively. Without loss of generality, we take $b_\mu = [b_0, b_1(y), b_2, b_3(t), 0]$ and A_μ the same as in Eq. (11). Defining the (pseudo-) magnetic and (pseudo-) electric fields as $\mathbf{B} = \nabla \times \mathbf{A}$ ($\mathbf{B}^5 = \nabla \times \mathbf{b}$), and $\mathbf{E} = \partial_t \mathbf{A} - \nabla A_0$ ($\mathbf{E}^5 = \partial_t \mathbf{b} - \nabla b_0$), respectively. We obtain the charge and valley currents,

$$J^w = \frac{C_{2v}}{2\pi^2} (E_z^5 B_z + E_z B_z^5), \tag{17a}$$

$$J_5^w = \frac{C_{2v}}{4\pi^2} (E_z B_z + E_z^5 B_z^5). \tag{17b}$$

Since the charge current J^w induced by a varying b_μ and magnetic (electric) field, we name it *valley-induced magnetic (electric) effect*. J_5^w is related to the 4D quantum valley Hall effect, where two valley Hall currents propagate along opposite directions.

We can also integrate J^w and J_5^w with respect to x, y and obtain

$$\int dxdy\, J^w = \frac{C_{2v}}{\pi} (N_{xy} E_z^5 + N_{xy}^5 E_z), \tag{18a}$$

$$\int dxdy\, J_5^w = \frac{C_{2v}}{2\pi} (N_{xy} E_z + N_{xy}^5 E_z^5), \tag{18b}$$

where $N_{xy}^5 = \int dxdy\, B_z^5/2\pi$ now denotes the number of pseudoflux quanta through the xy plane, which can be also quantized to be an integer as N_{xy}, mentioned above. The understanding of these terms will be similar to the case in Eq. (13). For instance, the second (first) term in Eq. (18a) could be treated as the (pseudo-) Hall effect with a quantized hall conductance $C_{2v}N_{xy}^5(N_{xy})/\pi$ in the zw plane induced by a pseudo-(usual) magnetic field with flux $2\pi N_{xy}^5(2\pi N_{xy})$ in the normal xy plane. Similarly, the (second) first term in Eq. (18b) represents the (pseudo-) valley Hall effect in the zw plane induced by a (pseudo-) usual magnetic field in the xy plane.

From the viewpoint of 3D boundary physics, b_μ splits a Dirac point into two Weyl points with opposite chirality separated in energy and in momentum, i.e., there are $|C_{2v}|$

pairs of Weyl points on the boundary. One can straightforwardly obtain the boundary effective action and the corresponding response currents from the bulk as we did above. It is possible to show that the 3D boundary supports topological responses upon applying EM, and pseudo-EM fields are the same as those derived from the 3D Weyl Hamiltonian, which has been widely studied in the previous work [62]. The boundary response is actually a signature of a bulk response. Interestingly, when b_μ is constant, we obtain nonzero chiral magnetic and anomalous Hall current in the 3D boundary even though the 4D bulk charge current is zero.

Topological phase transitions.—In the presence of Δ, the system $\mathcal{H}_1$ breaks all the symmetries and falls into class A. Even though each block subsystem breaks TRS, each of them is still a 4D QHI in class A which is quite robust and is characterized by the unchanged second CN $C_2^{\pm}$ and hosts nontrivial boundary modes. So the system continues to host a $\mathbb{Z}_2$ number until a topological phase transition occurs when the bulk gap closes with a critical value b_μ. This indicates a phase transition from a $\mathbb{Z}_2$ TI to a trivial insulator where the corresponding topological response predicted from Eqs. (17a) and (17b) also changes from nontrivial to trivial. Moreover, we can add a term $\Delta_a = cG_{302} + b_0 G_{332}$ to $\mathcal{H}_0$. The model now falls into class A and goes through a phase transition from a $\mathbb{Z}_2$ TI to a nontrivial DNL/NHT semimetallic phase and then finally becomes a trivial insulator by increasing $|c|$. Such a DNL structure is characterized by the first CN while a NHT is the 3D torus protected by the γ_5 symmetry associated with a 0D $\mathbb{Z}$-value number [39]. Furthermore, the term $\Delta_z = \delta_z G_{032}$ that will induce a phase transition from $\mathbb{Z}_2$ to $\mathbb{Z}$ TIs falls into class AII when $|\delta_z|$ is large enough. This term induces a very rich phase diagram that supports higher second CNs (e.g., $C_2 = \pm 2, \pm 4, \pm 6$) by varying m and δ_z [39].

Conclusion and outlook.—We have proposed a novel $\mathbb{Z}_2$ TI model characterized by a $\mathbb{Z}_2$ number ν_2 associated with the second spin (valley) CN, whose 3D boundaries support an odd number (pairs) of real Dirac (Weyl) points, and investigated its topology. In particular, we have revealed several new types of topological responses upon applying the EM and the pseudo-EM fields. Several external terms induce topological phase transitions and give rise to very rich phase diagrams. These topological quantum effects can also appear in the 4D $\mathbb{Z}_2$ TIs in class CII and C [39]. Note that the predicted responses could be experimental studied in 3D quantum-engineered setups extended by a synthetic or artificial dimension [63], as could be realized in the photonic or phononic crystals [7,8] where the pseudo-EM field can be induced by a strain field [64,65], in electric circuits [29,30], or in optical lattices with cold atoms [4,5,66,67], etc. In the Supplemental Material, we present an experimentally feasible proposal for realizing the $\mathbb{Z}_2$ TI model and detecting the predicted responses in a 3D optical lattice with an external periodic parameter using ultracold atoms [39]. These results may pave the way for exploring topological responses in the HDTPs and in artificial systems.

Finally, we note that topological crystalline [68,69] or higher-order topological phases [70,71] can be induced from $\mathcal{H}_0$ and the corresponding effective field-theoretical descriptions are worth exploring. By using the dimensional reduction method, one can explore the 2D $\mathbb{Z}_2$ pumping of $\mathcal{H}_0$, where ν_2 can be measured through the drift of the center of mass of atom clouds [72]. Besides, the investigation of a non-Hermitian 4D $\mathbb{Z}_2$ TI and its topological field theory [73,74] is also one of the possible directions. Moreover, some interesting physics in spin and anomalous planar Hall systems [75,76] can be generalized into four dimensions while our model with interacting may reveal more novel physics regarding the current progress [77–81].

This work was supported by the Key-Area Research and Development Program of Guangdong Province (Grant No. 2019B030330001), NSFC/RGC JRS Grant (N-HKU774/21), and the CRF of Hong Kong (C6009-20G).

*yqzhuphy@hku.hk
†giandomenico.palumbo@gmail.com
‡zwang@hku.hk

[1] M. Z. Hasan and C. L. Kane, Rev. Mod. Phys. **82**, 3045 (2010).
[2] X.-L. Qi and S.-C. Zhang, Rev. Mod. Phys. **83**, 1057 (2011).
[3] N. P. Armitage, E. J. Mele, and A. Vishwanath, Rev. Mod. Phys. **90**, 015001 (2018).
[4] D.-W. Zhang, Y.-Q. Zhu, Y. X. Zhao, H. Yan, and S.-L. Zhu, Adv. Phys. **67**, 253 (2018).
[5] N. R. Cooper, J. Dalibard, and I. B. Spielman, Rev. Mod. Phys. **91**, 015005 (2019).
[6] Y. Xu, Front. Phys. **14**, 43402 (2019).
[7] T. Ozawa, H. M. Price, A. Amo, N. Goldman, M. Hafezi, L. Lu, M. C. Rechtsman, D. Schuster, J. Simon, O. Zilberberg, and I. Carusotto, Rev. Mod. Phys. **91**, 015006 (2019).
[8] J. Liu, H. Guo, and T. Wang, Crystals **10**, 305 (2020).
[9] K. Landsteiner, Acta Phys. Pol. B **47**, 2617 (2016).
[10] X.-L. Qi, T. L. Hughes, and S.-C. Zhang, Phys. Rev. B **78**, 195424 (2008).
[11] G. Palumbo, R. Catenacci, and A. Marzuoli, Int. J. Mod. Phys. B **28**, 1350193 (2014).
[12] S. T. Ramamurthy, Y. Wang, and T. L. Hughes, Phys. Rev. Lett. **118**, 146602 (2017).
[13] S. T. Ramamurthy and T. L. Hughes, Phys. Rev. B **92**, 085105 (2015).
[14] A. G. Grushin, Phys. Rev. D **86**, 045001 (2012).
[15] M. M. Vazifeh and M. Franz, Phys. Rev. Lett. **111**, 027201 (2013).
[16] D. I. Pikulin, Anffany Chen, and M. Franz, Phys. Rev. X **6**, 041021 (2016).
[17] J. Behrends, S. Roy, M. H. Kolodrubetz, J. H. Bardarson, and A. G. Grushin, Phys. Rev. B **99**, 140201(R) (2019).
[18] R. A. Bertlmann, *Anomalies in Quantum Field Theory* (Oxford University Press, New York, 2000).

[19] Z. Lin, X.-J. Huang, D.-W. Zhang, S.-L. Zhu, and Z. D. Wang, Phys. Rev. A **99**, 043419 (2019).
[20] Y.-Q. Zhu, N. Goldman, and G. Palumbo, Phys. Rev. B **102**, 081109(R) (2020).
[21] A. A. Zyuzin and A. A. Burkov, Phys. Rev. B **86**, 115133 (2012).
[22] C.-X. Liu, P. Ye, and X.-L. Qi, Phys. Rev. B **87**, 235306 (2013).
[23] A. A. Burkov and Y. B. Kim, Phys. Rev. Lett. **117**, 136602 (2016).
[24] H. M. Price, O. Zilberberg, T. Ozawa, I. Carusotto, and N. Goldman, Phys. Rev. Lett. **115**, 195303 (2015).
[25] I. Petrides, H. M. Price, and O. Zilberberg, Phys. Rev. B **98**, 125431 (2018).
[26] C. H. Lee, Y. Wang, Y. Chen, and X. Zhang, Phys. Rev. B **98**, 094434 (2018).
[27] H. M. Price, Phys. Rev. B **101**, 205141 (2020).
[28] W. Cheng, E. Prodan, and C. Prodan, Phys. Rev. Appl. **16**, 044032 (2021).
[29] Y. Wang, H. M. Price, B. Zhang, and Y. D. Chong, Nat. Commun. **11**, 2356 (2020).
[30] L. Li, C. H. Lee, and J. Gong, Commun. Phys. **2**, 135 (2019).
[31] C.-K. Chiu, J. C. Y. Teo, A. P. Schnyder, and S. Ryu, Rev. Mod. Phys. **88**, 035005 (2016).
[32] H. Shapourian, T. L. Hughes, and S. Ryu, Phys. Rev. B **92**, 165131 (2015).
[33] A. Cortijo, Y. Ferreirós, K. Landsteiner, and M. A. H. Vozmediano, Phys. Rev. Lett. **115**, 177202 (2015).
[34] A. G. Grushin, J. W. F. Venderbos, A. Vishwanath, and R. Ilan, Phys. Rev. X **6**, 041046 (2016).
[35] The matrices are given by $\Gamma_1 = \sigma_1 \otimes \sigma_0 \otimes \sigma_1$, $\Gamma_2 = \sigma_1 \otimes \sigma_2 \otimes \sigma_2$, $\Gamma_3 = \sigma_1 \otimes \sigma_0 \otimes \sigma_3$, $\Gamma_4 = \sigma_1 \otimes \sigma_1 \otimes \sigma_2$, and $\Gamma_0 = \sigma_3 \otimes \sigma_0 \otimes \sigma_0$.
[36] Y. X. Zhao, A. P. Schnyder, and Z. D. Wang, Phys. Rev. Lett. **116**, 156402 (2016).
[37] I. Petrides and O. Zilberberg, arXiv:2203.14902.
[38] The $\mathbb{Z}_2$ number can be also defined as

$$\nu_2 = \frac{\pi^2}{15}\int \frac{d\omega d^4k}{(2\pi)^5}\epsilon^{\mu\nu\lambda\rho\sigma}\mathrm{tr}\left[\frac{\Gamma_5}{2}G\partial_{k_\mu}G^{-1}G\partial_{k_\nu}G^{-1} \times G\partial_{k_\lambda}G^{-1}G\partial_{k_\rho}G^{-1}G\partial_{k_\sigma}G^{-1}\right] \mathrm{mod}\ 2,$$

with the imaginary Green function $G(\omega,k)^{-1} = i\omega - \mathcal{H}_0(k)$. After rotating $\mathcal{H}_0$ into the block diagonal form and substituting the relation $G^{-1} = U^{-1}G_{BD}^{-1}U = U^{-1}(i\omega - \mathcal{H}_{BD})U$ into ν_2, we obtain the expression as in Eq. (4) where $C_2^{\pm}$ is now expressed in terms of the imaginary Green function and is equivalent to the expression associated with the non-Ableian Berry curvature [10].
[39] See Supplemental Material at http://link.aps.org/supplemental/10.1103/PhysRevLett.129.196602 for details, which includes Refs. [40–52].
[40] L. B. Shao and Y. X. Zhao, arXiv:1805.07323v1.
[41] J.-X. Dai, K. Wang, S. A. Yang, and Y. X. Zhao, Phys. Rev. B **104**, 165142 (2021).
[42] G. Palumbo, Phys. Rev. Lett. **126**, 246801 (2021).
[43] M. E. Peskin and D. V. Schroeder, *An Introduction to Quantum Field Theory* (Addison-Wesley Publishing Company, Massachusetts, 1995).
[44] A. Zee, *Quantum Field Theory in a Nutshell* (Princeton University Press, New Jersey, 2010).
[45] Y. Yang, Z. Xu, L. Sheng, B. Wang, D. Y. Xing, and D. N. Sheng, Phys. Rev. Lett. **107**, 066602 (2011).
[46] M. Takamoto and H. Katori, Phys. Rev. Lett. **91**, 223001 (2003).
[47] Z.-Y. Wang, X.-C. Cheng, B.-Z. Wang, J.-Y. Zhang, Y.-H. Lu, C.-R. Yi, S. Niu, Y. Deng, X.-J. Liu, S. Chen, and J.-W. Pan, Science **372**, 271 (2021).
[48] A. V. Gorshkov, M. Hermele, V. Gurarie, C. Xu, P. S. Julienne, J. Ye, P. Zoller, E. Demler, M. D. Lukin, and A. M. Rey, Nat. Phys. **6**, 289 (2010).
[49] J. Dalibard, F. Gerbier, G. Juzeliūnas, and P. Öhberg, Rev. Mod. Phys. **83**, 1523 (2011).
[50] N. Goldman, G. Juzeliūnas, P. Öhberg, and I. B. Spielman, Rep. Prog. Phys. **77**, 126401 (2014).
[51] H. M. Price, O. Zilberberg, T. Ozawa, I. Carusotto, and N. Goldman, Phys. Rev. B **93**, 245113 (2016).
[52] M. Kolodrubetz, Phys. Rev. Lett. **117**, 015301 (2016).
[53] Y. X. Zhao and Y. Lu, Phys. Rev. Lett. **118**, 056401 (2017).
[54] J. Ahn, D. Kim, Y. Kim, and B.-J. Yang, Phys. Rev. Lett. **121**, 106403 (2018).
[55] F. N. Ünal, A. Bouhon, and R.-J. Slager, Phys. Rev. Lett. **125**, 053601 (2020).
[56] A. Bouhon, Q. Wu, R.-J. Slager, H. Weng, O. V. Yazyev, and T. Bzdušek, Nat. Phys. **16**, 1137 (2020).
[57] The block diagonal Hamiltonian reads $u\mathcal{H}_{RD}u^{-1} = \mathcal{H}_W^+ \oplus \mathcal{H}_W^-$, with $u = \exp[-i(\pi/4)G_{10}]\exp[i(\pi/4)G_{12}]$. Here $\mathcal{H}_W^{\pm} = k_x\sigma_1 \pm k_y\sigma_2 - k_z\sigma_3 = \sum_{i,j} v_{ij}^{\pm}k_i\sigma_j$. The chirality can be verified as $\eta_{\pm} = \mathrm{sign}(\det v_{ij}^{\pm}) = \mp 1$.
[58] O. Türker and S. Moroz, Phys. Rev. B **97**, 075120 (2018).
[59] G. Salerno, N. Goldman, and G. Palumbo, Phys. Rev. Res. **2**, 013224 (2020).
[60] In the region $0 < m < 2[-2 < m < 0]$, there are three real Dirac points (or three pairs of Weyl points) that survive on the 3D boundary near three high symmetry points $(\pi,0,0)[(\pi,\pi,0)]$, $(0,\pi,0)[(\pi,0,\pi)]$, $(0,0,\pi)[(0,\pi,\pi)]$, respectively. In the region $-4 < m < -2$, a real Dirac point (or a pair of Weyl points) survives on the 3D boundary near (π,π,π).
[61] In Ref. [20], the authors study the parity anomaly in a 4D semimetal with two monopoles separated by the b_μ field. In fact, there is an extra nonzero term $b_\mu\partial_\nu b_\lambda\partial_\rho b_\sigma$ in the topological action which has been safely neglected since they only mention the charge current in their work. In this Letter, we obtain the similar action in Eq. (10) by just replacing b_μ with $\tilde{A}_\mu$ after performing a diagrammatic calculation in the supplemental material of Ref. [20].
[62] R. Ilan, A. G. Grushin, and D. I. Pikulin, Nat. Rev. Phys. **2**, 29 (2020).
[63] T. Ozawa and H. M. Price, Nat. Rev. Phys. **1**, 349 (2019).
[64] M. C. Rechtsman, J. M. Zeuner, A. Tunnermann, S. Nolte, M. Segev, and A. Szameit, Nat. Photonics **7**, 153 (2013).
[65] Z. Yang, F. Gao, Y. Yang, and B. Zhang, Phys. Rev. Lett. **118**, 194301 (2017).
[66] Z. Zheng, Z. Lin, D.-W. Zhang, S.-L. Zhu, and Z. D. Wang, Phys. Rev. Res. **1**, 033102 (2019).

[67] M. Jamotte, N. Goldman, and M. Di Liberto, Commun. Phys. **5**, 30 (2022).
[68] L. Fu, Phys. Rev. Lett. **106**, 106802 (2011).
[69] R.-J. Slager, A. Mesaros, V. Juričić, and J. Zaanen, Nat. Phys. **9**, 98 (2013).
[70] B. J. Wieder, Z. Wang, J. Cano, X. Dai, L. M. Schoop, B. Bradlyn, and B. A. Bernevig, Nat. Commun. **11**, 627 (2020).
[71] F. Schindler, A. M. Cook, M. G. Vergniory, Z. Wang, S. S. P. Parkin, B. Andrei Bernevig, and T. Neupert, Sci. Adv. **4**, eaat0346 (2018).
[72] M. Lohse, C. Schweizer, H. M. Price, O. Zilberberg, and I. Bloch, Nature (London) **553**, 55 (2018).
[73] K. Kawabata, K. Shiozaki, and S. Ryu, Phys. Rev. Lett. **126**, 216405 (2021).
[74] S. Sayyad, J. D. Hannukainen, and A. G. Grushin, Phys. Rev. Res. **4**, L042004 (2022).
[75] P. Bhalla, M.-X. Deng, R.-Q. Wang, L. Wang, and D. Culcer, Phys. Rev. Lett. **127**, 206801 (2021).
[76] J. H. Cullen, P. Bhalla, E. Marcellina, A. R. Hamilton, and D. Culcer, Phys. Rev. Lett. **126**, 256601 (2021).
[77] A. Marzuoli and G. Palumbo, Europhys. Lett. **99**, 10002 (2012).
[78] G. Palumbo and J. K. Pachos, Phys. Rev. Lett. **110**, 211603 (2013).
[79] G. Palumbo and J. K. Pachos, Phys. Rev. D **90**, 027703 (2014).
[80] M. Cirio, G. Palumbo, and J. K. Pachos, Phys. Rev. B **90**, 085114 (2014).
[81] C. Rylands, A. Parhizkar, A. A. Burkov, and V. Galitski, Phys. Rev. Lett. **126**, 185303 (2021).